

Magneto-optical effect of left-handed material

H.X. Da^{1,a}, C. Xu^{1,3}, and Z.Y. Li^{2,1}

¹ Department of Physics, Suzhou University, Suzhou 215006, China

² CCAST (World Laboratory), P.O. Box 8730, Beijing 100080, China

³ National Laboratory of Solid State Microstructures, Nanjing University, Nanjing 215006, China

Received 20 January 2005

Published online 6 July 2005 – © EDP Sciences, Società Italiana di Fisica, Springer-Verlag 2005

Abstract. In this paper, we suggest a possibility of providing left-handed material with parallel ferromagnetic nanowires electrodeposited into an insulating polycarbonate membrane. We find that such a composite shows left-handed properties when the damping factor α satisfies $\alpha < \alpha_c$, where α_c is the critical damping factor which is affected by the filling factor of ferromagnetic nanowires. We also investigate the magneto-optical properties of such a composite and find that at the frequency region where the composite exhibits left-handed property, both the Faraday rotation angle and ellipticity of the film show obvious change apart from a jump in transmission coefficient at the frequency region near the ferromagnetic resonance frequency. Compared with the pure ferromagnetic film, a larger Faraday rotation angle is obtained in our model, which may be useful for the application of magneto-optical devices.

PACS. 42.70.Qs Photonic bandgap materials – 73.20.Mf Collective excitations (including excitons, polarons, plasmons and other charge-density excitations) – 78.20.Ls Magneto-optical effects

1 Introduction

Magneto-optical properties have aroused considerable interest as a powerful tool for investigating the characters of magnetic materials. They have been extensively studied in magnetic thin films [1, 2], composites of small particles [3, 4] and magnetic fluids [5, 6]. The characters of the interaction between the applied polarized light and the magnetic material are presented by the change in the state of light polarization, both in transmission (Faraday rotation effect) and reflection (Kerr effect). When a linearly polarized beam with a parallel magnetic field impinges on a magnetic material, the beam will experience different refractive indices and thus travel with different speeds in the material due to the differences between left and right circular polarization. Thus, the outgoing refractive beam will rotate an angle relative to the incident beam, which is generally known as Faraday rotation. One particular interest is the magneto-optical effects in multilayered structures consisting of thin rare-earth iron garnet magnetic layers, for example, usually using Bi-Substituted YIG (Bi:YIG) or Co etc in magnetophotonic crystal, high transmittance and a large Faraday rotation angle can be obtained due to the localization effect of light [7–9]. Compared with single magnetic layer, the whole thickness of multilayered structures is smaller than that of single bulk magnetic material, which makes it a good candidate in magneto-optical memory media applications [7].

Recently, due to the realization of left-handed materials in experiments, the studies on left-handed material

are sky-rocketing. These novel materials with simultaneously negative dielectric permittivity ϵ and magnetic permeability μ show many different behaviors from conventional materials, such as anomalous refraction, the reversal of Doppler effect and Cerenkov radiation [10–12]. When an electromagnetic wave propagates in such media, its propagation direction will be opposite to its energy flow direction. Smith et al. [10] constructed the composite with intercalating arrays of wires and split-ring resonators and found both the effective dielectric permittivity and magnetic permeability of such a composite are negative when the applied electromagnetic wave is at a certain microwave frequency region. In addition, Chui et al. [13, 14] advanced a possibility of preparing left-handed material by incorporating metallic ferromagnetic nanoparticles into an appropriate insulating matrix when electromagnetic wave propagates in some special direction and polarization at a frequency region near the ferromagnetic resonance frequency. Wu et al. [15] investigated the high-frequency response of a fully magnetized metallic film with magnetization perpendicular to the film surface. They demonstrated that the magnetic film exhibits left-handed characteristics at a certain frequency region and showed that the frequency region of left-handed properties is related with the damping coefficient directly, which is manifested with a jump in transmission coefficient at the frequency region near the ferromagnetic resonance frequency. In consequence of the inherent large conductivity of ferromagnetic film which may lead to the difficulty in technical application, we suggest a possibility of providing left-handed material with a composite composed of parallel ferromagnetic

^a e-mail: haixia8779@163.com

nanowires electrodeposited into an insulating polycarbonate membrane. Our results show that the composite shows left-handed properties at a certain frequency region when the damping factor α satisfies $\alpha < \alpha_c$, where α_c is the critical damping factor which is affected by the filling factor of ferromagnetic nanowires.

This kind of left-handed material is usually magnetic anisotropic in nature, then what is the case of the magneto-optical effect in such a left-handed material? To clarify this, we investigate the magneto-optical properties of the left-handed material by 4×4 transfer matrix method [16,17] in this paper. This method is widely used to investigate the magneto-optical effect in biaxial crystal, magnetophotonic crystal [7–9]. Compared with a pure ferromagnetic film, a larger Faraday rotation angle is obtained in our model, which may be useful for the application of magneto-optical devices. The influence of the film thickness on the Faraday rotation angle is also investigated. Our results show that the thinner the film is, the larger the Faraday rotation angle will be.

2 Transfer matrix method

A simple case of an anisotropic layer is depicted in Figure 1a. The incident electromagnetic wave propagates along the z -direction with the electric field polarized along the x -direction and the magnetic field polarized along y -direction. We will derive the Faraday rotation angle and ellipticity of arbitrary anisotropic magnetic material by using the 4×4 transfer matrix method. This method relates one side of a structure to the other. Although now we just discuss a single layer, it is easy to extend such a single layer structure into multilayered structures. The fundamental wave equations are given by Maxwell's equations:

$$\begin{aligned}\nabla \times \vec{E}(\vec{r}, t) &= i\omega\mu_0\tilde{\mu}\vec{H}(\vec{r}, t), \\ \nabla \times \vec{H}(\vec{r}, t) &= -i\omega\varepsilon_0\tilde{\varepsilon}\vec{E}(\vec{r}, t).\end{aligned}\quad (1)$$

The dielectric permittivity and magnetic permeability tensors in equation (1) are expressed as

$$\begin{aligned}\tilde{\varepsilon} &= \begin{pmatrix} \varepsilon_1 & i\varepsilon_2 & 0 \\ -i\varepsilon_2 & \varepsilon_1 & 0 \\ 0 & 0 & \varepsilon_3 \end{pmatrix}, \\ \tilde{\mu} &= \begin{pmatrix} \mu_1 & i\mu_2 & 0 \\ -i\mu_2 & \mu_1 & 0 \\ 0 & 0 & \mu_3 \end{pmatrix}.\end{aligned}\quad (2)$$

Here we would like to note that the general expressions of the 4×4 transfer matrix method can be found elsewhere [7,16,17], however they were mostly concerned with the optical frequency region, where the permeability is usually taken to 1. With the realization of left-handed material at the microwave frequency region, the role of permeability becomes important. Therefore, it is necessary for us to extend the previous formulae into more generalized ones. We mainly adopt the method provided by references [16] and [17]. The state of the

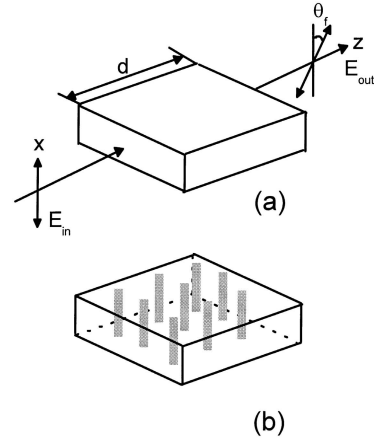


Fig. 1. (a) Geometrical structure of the problem. (b) Our composite: the array of magnetic nanowires embedded in the polymer membrane.

incident wave travelling the magnetic layer is denoted as a column vector of $\Phi = \{e_x, e_y, h_x, h_y\}^t$, where e_x , e_y , h_x , and h_y stand for the components of the electric field $e(= \varepsilon_0 E)$ and magnetic field $h(= \mu_0 H/c)$, respectively. The superscript t denotes the transpose operator. ε_0 , μ_0 , and c are the dielectric permittivity, magnetic permeability, and light velocity of vacuum, respectively. The state of the incident wave can be described as:

$$\begin{aligned}\Phi(z) &= \begin{bmatrix} e_x \\ e_y \\ h_x \\ h_y \end{bmatrix} = A \begin{bmatrix} 1 \\ -i \\ i\sqrt{\frac{\varepsilon_1 + \varepsilon_2}{\mu_1 + \mu_2}} \\ \sqrt{\frac{\varepsilon_1 + \varepsilon_2}{\mu_1 + \mu_2}} \end{bmatrix} e^{ik_1 z} \\ &+ B \begin{bmatrix} 1 \\ -i \\ -i\sqrt{\frac{\varepsilon_1 + \varepsilon_2}{\mu_1 + \mu_2}} \\ -\sqrt{\frac{\varepsilon_1 + \varepsilon_2}{\mu_1 + \mu_2}} \end{bmatrix} e^{-ik_1 z} + C \begin{bmatrix} 1 \\ i \\ -i\sqrt{\frac{\varepsilon_1 - \varepsilon_2}{\mu_1 - \mu_2}} \\ \sqrt{\frac{\varepsilon_1 - \varepsilon_2}{\mu_1 - \mu_2}} \end{bmatrix} e^{ik_2 z} \\ &+ D \begin{bmatrix} 1 \\ i \\ i\sqrt{\frac{\varepsilon_1 - \varepsilon_2}{\mu_1 - \mu_2}} \\ -\sqrt{\frac{\varepsilon_1 - \varepsilon_2}{\mu_1 - \mu_2}} \end{bmatrix} e^{-ik_2 z},\end{aligned}\quad (3)$$

where $k_1 = \frac{\omega}{c}\sqrt{(\varepsilon_1 + \varepsilon_2)(\mu_1 + \mu_2)}$ and $k_2 = \frac{\omega}{c}\sqrt{(\varepsilon_1 - \varepsilon_2)(\mu_1 - \mu_2)}$. k_1 and k_2 are the wave vectors of right and left circular polarization, respectively. A , B , C , and D are the coupling coefficients, which can be uniquely related to the four transverse field components (e_x, e_y, h_x, h_y) at a given z [10,11]. The four eigenmodes from equation (3) are the

column vectors as $\begin{bmatrix} 1 - i i \sqrt{\frac{\varepsilon_1 + \varepsilon_2}{\mu_1 + \mu_2}} \sqrt{\frac{\varepsilon_1 + \varepsilon_2}{\mu_1 + \mu_2}} \end{bmatrix}^t e^{ik_1 z}$, $\begin{bmatrix} 1 - i - i \sqrt{\frac{\varepsilon_1 + \varepsilon_2}{\mu_1 + \mu_2}} - \sqrt{\frac{\varepsilon_1 + \varepsilon_2}{\mu_1 + \mu_2}} \end{bmatrix}^t e^{-ik_1 z}$, $\begin{bmatrix} 1 i - i \sqrt{\frac{\varepsilon_1 - \varepsilon_2}{\mu_1 - \mu_2}} \sqrt{\frac{\varepsilon_1 - \varepsilon_2}{\mu_1 - \mu_2}} \end{bmatrix}^t e^{ik_2 z}$, and $\begin{bmatrix} 1 i i \sqrt{\frac{\varepsilon_1 - \varepsilon_2}{\mu_1 - \mu_2}} - \sqrt{\frac{\varepsilon_1 - \varepsilon_2}{\mu_1 - \mu_2}} \end{bmatrix}^t e^{-ik_2 z}$. In accordance with these eigenmodes, we may get the transfer matrix of the magnetic layer. Then the elements of the transfer matrix are given by:

$$\begin{aligned}
t_{11} &= \frac{1}{2} (\cos \delta_1 + \cos \delta_2) \\
t_{21} &= \frac{i}{2} (-\cos \delta_1 + \cos \delta_2) \\
t_{31} &= \frac{1}{2} \left(-\sqrt{\frac{\varepsilon_1 + \varepsilon_2}{\mu_1 + \mu_2}} \sin \delta_1 + \sqrt{\frac{\varepsilon_1 - \varepsilon_2}{\mu_1 - \mu_2}} \sin \delta_2 \right) \\
t_{41} &= \frac{i}{2} \left(\sqrt{\frac{\varepsilon_1 + \varepsilon_2}{\mu_1 + \mu_2}} \sin \delta_1 + \sqrt{\frac{\varepsilon_1 - \varepsilon_2}{\mu_1 - \mu_2}} \sin \delta_2 \right) \\
t_{12} &= \frac{i}{2} (\cos \delta_1 - \cos \delta_2) \\
t_{22} &= \frac{1}{2} (\cos \delta_1 + \cos \delta_2) \\
t_{32} &= -\frac{i}{2} \left(\sqrt{\frac{\varepsilon_1 + \varepsilon_2}{\mu_1 + \mu_2}} \sin \delta_1 + \sqrt{\frac{\varepsilon_1 - \varepsilon_2}{\mu_1 - \mu_2}} \sin \delta_2 \right) \\
t_{42} &= \frac{1}{2} \left(-\sqrt{\frac{\varepsilon_1 + \varepsilon_2}{\mu_1 + \mu_2}} \sin \delta_1 + \sqrt{\frac{\varepsilon_1 - \varepsilon_2}{\mu_1 - \mu_2}} \sin \delta_2 \right) \\
t_{13} &= \frac{1}{2} \left(\sqrt{\frac{\mu_1 + \mu_2}{\varepsilon_1 + \varepsilon_2}} \sin \delta_1 - \sqrt{\frac{\mu_1 - \mu_2}{\varepsilon_1 - \varepsilon_2}} \sin \delta_2 \right) \\
t_{23} &= -\frac{i}{2} \left(\sqrt{\frac{\mu_1 + \mu_2}{\varepsilon_1 + \varepsilon_2}} \sin \delta_1 + \sqrt{\frac{\mu_1 - \mu_2}{\varepsilon_1 - \varepsilon_2}} \sin \delta_2 \right) \\
t_{33} &= \frac{1}{2} (\cos \delta_1 + \cos \delta_2) \\
t_{43} &= \frac{i}{2} (-\cos \delta_1 + \cos \delta_2) \\
t_{14} &= \frac{i}{2} \left(\sqrt{\frac{\mu_1 + \mu_2}{\varepsilon_1 + \varepsilon_2}} \sin \delta_1 + \sqrt{\frac{\mu_1 - \mu_2}{\varepsilon_1 - \varepsilon_2}} \sin \delta_2 \right) \\
t_{24} &= \frac{1}{2} \left(\sqrt{\frac{\mu_1 + \mu_2}{\varepsilon_1 + \varepsilon_2}} \sin \delta_1 - \sqrt{\frac{\mu_1 - \mu_2}{\varepsilon_1 - \varepsilon_2}} \sin \delta_2 \right) \\
t_{34} &= \frac{i}{2} (\cos \delta_1 - \cos \delta_2) \\
t_{44} &= \frac{1}{2} (\cos \delta_1 + \cos \delta_2)
\end{aligned} \tag{4}$$

with $\delta_1 = k_1 d$ and $\delta_2 = k_2 d$, where d is the thickness of the layer. If the magnetic layer occupies the spatial region of $z_0 < z < z_0 + d$, the transmission characteristics of the magnetic layer can be given by using the following equation

$$\Phi(z_0 + d) = T\Phi(z_0) \tag{5}$$

where T is the transfer matrix with its elements given by equation (4), i.e., when the electromagnetic wave is incident normally to the magnetic film surface, the state vector in the $z < z_0$ is given by the sum of the ingoing TM wave and the reflected TM and TE wave, and the state vector in the $z > z_0 + d$ is given by the sum of the outgoing TM and TE wave. If we express them in the form of matrix, the state of output electromagnetic wave is given by [9]

$$\begin{pmatrix} t_1 & 0 & 0 & 0 \\ 0 & 0 & t_2 & 0 \\ 0 & 0 & -t_2 & 0 \\ t_1 & 0 & 0 & 0 \end{pmatrix} \begin{pmatrix} e^{ik(z-z_0-d)} \\ e^{-ik(z-z_0-d)} \\ e^{ik(z-z_0-d)} \\ e^{-ik(z-z_0-d)} \end{pmatrix}_{z=z_0+d} = T \begin{pmatrix} 1 & r_1 & 0 & 0 \\ 0 & 0 & 0 & r_2 \\ 0 & 0 & 0 & r_2 \\ 1 & -r_1 & 0 & 0 \end{pmatrix} \begin{pmatrix} e^{ik(z-z_0)} \\ e^{-ik(z-z_0)} \\ e^{ik(z-z_0)} \\ e^{-ik(z-z_0)} \end{pmatrix}_{z=z_0} \tag{6}$$

where r_1 (r_2) denotes the reflectance of TM (TE) wave, t_1 (t_2) denotes the transmittance of TM (TE) wave, respectively. Thus for a given incident wave, the state at $z < z_0$ and the state at $z > z_0 + d$ will satisfy the following relation [7]

$$\begin{pmatrix} t_{11} - t_{14} & t_{12} + t_{13} & -1 & 0 \\ t_{21} - t_{24} & t_{22} + t_{23} & 0 & -1 \\ t_{31} - t_{34} & t_{32} + t_{33} & 0 & 1 \\ t_{41} - t_{44} & t_{42} + t_{43} & -1 & 0 \end{pmatrix} \begin{pmatrix} r_1 \\ r_2 \\ t_1 \\ t_2 \end{pmatrix} = - \begin{pmatrix} t_{11} + t_{14} \\ t_{21} + t_{24} \\ t_{31} + t_{34} \\ t_{41} + t_{44} \end{pmatrix}. \tag{7}$$

The reflectance and transmittance of the electromagnetic wave can be directly obtained from matrix equation (7). After getting the coefficients t_1 and t_2 , the Faraday rotation angle θ_f and the Faraday rotation ellipticity η_f can be therefore calculated by the following equations [7]:

$$\begin{aligned}
\theta_f &= \frac{1}{2d} \arctan \left(\frac{2\text{Re}(\chi)}{1 - |\chi|^2} \right) \\
\eta_f &= \frac{1}{d} \tan \left[\frac{1}{2} \arcsin \left(-\frac{2\text{Im}(\chi)}{1 + |\chi|^2} \right) \right]
\end{aligned} \tag{8}$$

where $\chi = \frac{t_2}{t_1}$.

3 Model and calculations

3.1 Left-handed property

A periodic arrays of magnetic nanowires synthesized by electrodeposition into templates have been investigated intensively in various areas such as giant magnetoresistance, magnetization reversal in a single nanowire [18–20].

However, possible left-handed property of such a system has not been reported so far. In this section, we consider a composite layer composed of parallel ferromagnetic nanowires electrodeposited into an insulating polycarbonate membrane, which is shown in Figure 1b. The dielectric permittivity and magnetic permeability of the nonmagnetic host are both scalar, which are denoted as ε_d and μ_d . The permittivity and permeability of metallic magnetic nanowires are expressed by

$$\tilde{\varepsilon}_f = \begin{pmatrix} \varepsilon_f & 0 & 0 \\ 0 & \varepsilon_f & 0 \\ 0 & 0 & \varepsilon_f \end{pmatrix}$$

$$\tilde{\mu}_f = \begin{pmatrix} \mu_{f1} & i\mu_{f2} & 0 \\ -i\mu_{f2} & \mu_{f1} & 0 \\ 0 & 0 & 1 \end{pmatrix} \quad (9)$$

with $\varepsilon_f = 1 - \frac{\omega_p^2}{\omega(\omega - i\kappa)}$, $\mu_{f1} = 1 + \frac{\omega_m(\omega_0 + i\alpha\omega)}{(\omega_0 + i\alpha\omega)^2 - \omega^2}$, and $\mu_{f2} = \frac{\omega_m\omega}{(\omega_0 + i\alpha\omega)^2 - \omega^2}$, where ω_p is the plasma frequency and κ is the electron damping factor, the ferromagnetic resonance frequency is $\omega_0 = \gamma H_0$ and the characteristic frequency is $\omega_m = \gamma M_s$. γ , M_s , and H_0 are the gyromagnetic ratio, the saturation magnetization and the effective magnetic field, respectively. α is the damping factor, which is directly in correlation with the condition for the layer exhibiting left-handed properties we will demonstrate later. Such a layer, as a whole, can be described by an effective layer with the effective permittivity and the tensor magnetic permeability. Then the permittivity and permeability of the composite layer are expressed by

$$\tilde{\varepsilon} = \begin{pmatrix} \varepsilon & 0 & 0 \\ 0 & \varepsilon & 0 \\ 0 & 0 & \varepsilon \end{pmatrix}$$

$$\tilde{\mu} = \begin{pmatrix} \mu_1 & i\mu_2 & 0 \\ -i\mu_2 & \mu_1 & 0 \\ 0 & 0 & \mu_3 \end{pmatrix} \quad (10)$$

where ε , μ_1 , and μ_2 can be obtained by using Maxwell-Garnett approximation [21–23] with these formulae:

$$\varepsilon = \varepsilon_f p + \varepsilon_d(1 - p)$$

$$\mu_1 = \mu_d + 2p\mu_d \frac{(\mu_{f1} - \mu_d)(\mu_{f1} + \mu_d) - \mu_{f2}^2}{(\mu_{f1} + \mu_d + \mu_{f2})(\mu_{f1} + \mu_d - \mu_{f2})}$$

$$\mu_2 = \frac{4p\mu_d^2\mu_{f2}}{(\mu_{f1} + \mu_d + \mu_{f2})(\mu_{f1} + \mu_d - \mu_{f2})} \quad (11)$$

where p is the filling fraction of ferromagnetic nanowires. Due to the character of lossy, the effective wave vectors of right (denoted by k_1) and left (denoted by k_2) circular polarization can be expressed as $k_{1,2} = \text{Re}[k_{1,2}] + i\text{Im}[k_{1,2}]$. The electric and magnetic fields in the composite can be described as $\vec{E}(\vec{r}, t) = \vec{E}^{\pm} e^{-i\text{Re}[k_{1,2}]z + \text{Im}[k_{1,2}]z + i\omega t}$ and $\vec{H}(\vec{r}, t) = \vec{H}^{\pm} e^{-i\text{Re}[k_{1,2}]z + \text{Im}[k_{1,2}]z + i\omega t}$, where \vec{E}^{\pm}

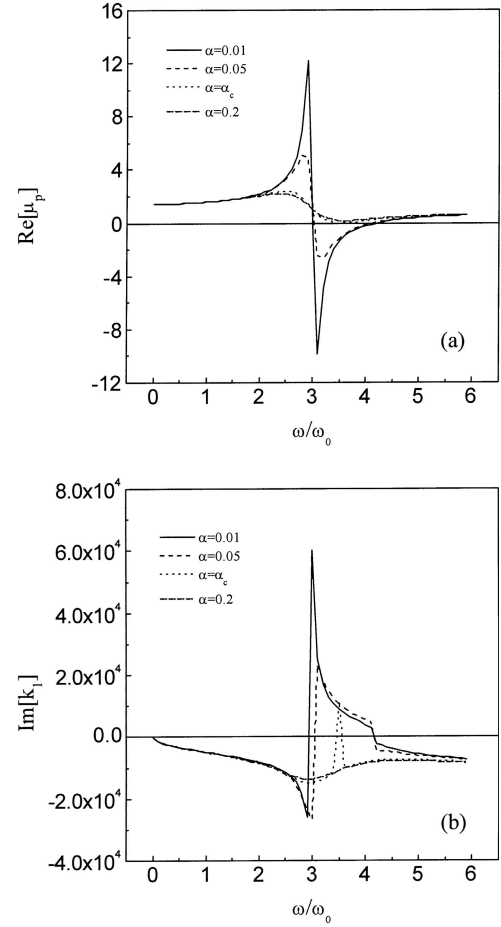


Fig. 2. (a) The real part of the permeability μ_p versus the relative frequency ω/ω_0 at the different damping factors $\alpha = 0.01, 0.05, \alpha_c$, and 0.2 . (b) The imaginary part of the wave vector k_1 of the right circular polarization at $\alpha = 0.01, 0.05, \alpha_c$, and 0.2 .

and \vec{H}^{\pm} denote the electric and magnetic fields for the right and left circular polarized waves, respectively. Negative imaginary part of the wave vector is used to ensure the energy flow in the positive direction [15]. The sign change of the imaginary part of the wave vector $k_{1,2}$ leads to the direction's change of the phase velocity, which means the left-handed property of the material. We take the parameters of the ferromagnetic nanowires material as those in reference [9], i.e., $\tilde{\omega}_m = \omega_m/\omega_0 = 4$, $\tilde{\omega}_p = \omega_p/\omega_0 = 10^6$, $\kappa = \tilde{\omega}_p/100$ and $\varepsilon_d = 2.89$, $\mu_d = 1$. For left circular polarization, we find that the real part of permeability ($\mu_1 - \mu_2$) is always positive, whereas, it is not true for the case of right circular polarization. Figure 2a gives the real part of the permeability ($\mu_p = \mu_1 + \mu_2$) and Figure 2b gives the imaginary part of the wave vector k_1 of right circular polarization for different damping factors. Inspection of Figure 2 shows that when the damping factor α is smaller than the critical value α_c , the real part of the permeability for right circular polarization is negative at a certain frequency region. The sign of $\text{Im}[k_1]$ changes at the same frequency region, which shows the composite layer

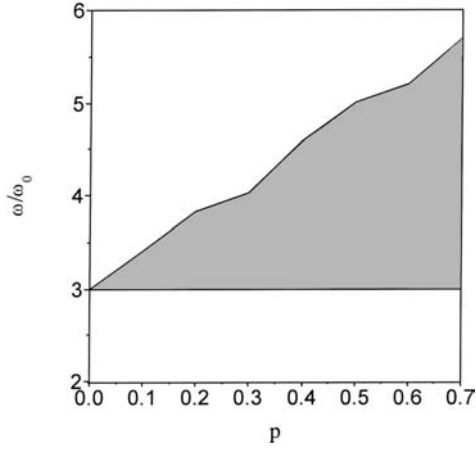


Fig. 3. The frequency region where the material shows left-handed property versus the filling factor at a given $\alpha = 0.01$.

exhibits left handed property for right circular polarization. α_c can be determined by using the condition that the real part of the permeability for right circular polarization equals to zero, i.e., $\mu_d + 2p\mu_d \frac{[\mu_{f1}^2 - (\mu_d - \mu_{f2})^2]}{(\mu_{f1} + \mu_d + \mu_{f2})(\mu_{f1} + \mu_d - \mu_{f2})} = 0$. We get $\alpha_c = 0.1688$ when the filling fraction p equals to 0.3. Obviously, the filling fraction will affect the value of the damping factor which determines the frequency region where the composite is left-handed. For a given α , the range of frequency that exhibits the left-handed property of a composite becomes wider with the increase of p . The shade region in Figure 3 shows the dependence of frequency region where the composite exhibits the left-handed property on p when $\alpha = 0.01$. It is obvious that the increase of the filling fraction widens the frequency region at which the composite shows the left-handed property. However we should note that high filling fraction of ferromagnetic nanowires leads to great energy losses. In practice, one needs to choose a proper p so as to get a relatively wide frequency region where the composite exhibits the left-handed property and low energy losses simultaneously. To get a relatively wide frequency region of left-handed properties with less energy losses, we take p as 0.3 in our calculations. Therefore, the insulating nature of the composite reduces the energy losses. Our results show that it is possible to realize left-handed material using a composite slab with parallel ferromagnetic nanowires electrodeposited into an insulating polycarbonate membrane at the frequency region near the ferromagnetic resonance frequency when electromagnetic wave propagates in some special direction.

3.2 Magneto-optical effect

In this section, we investigate the magneto-optical effect of the ferromagnetic composite that we defined in Figure 1b when electromagnetic wave propagates through it. Using equation (8), we can easily obtain the Faraday rotation angles and the Faraday rotation ellipticity. Figure 4 shows the Faraday rotation angles and the Faraday rotation ellipticity versus the the relative frequency ω/ω_0 . We can

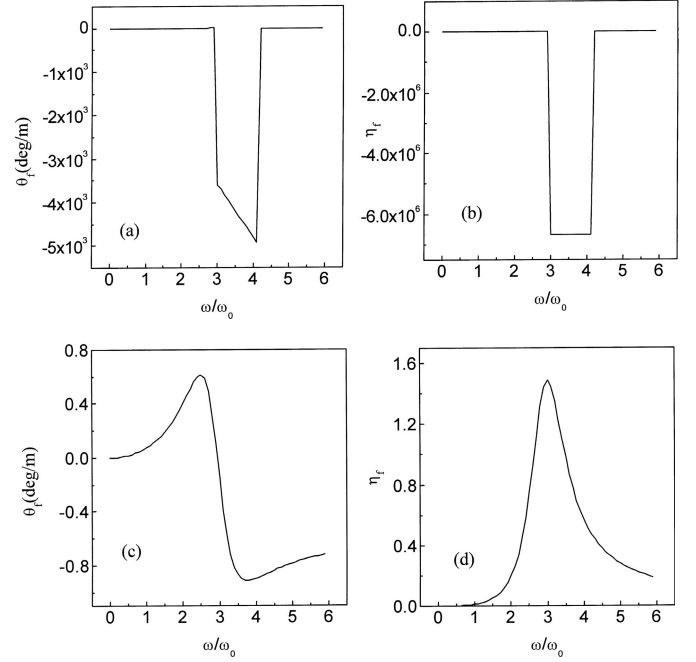


Fig. 4. (a) Dependence of the Faraday rotation angle on the relative frequency ω/ω_0 at $\alpha = 0.01$. (b) Dependence of the Faraday rotation ellipticity on the relative frequency ω/ω_0 at $\alpha = 0.01$. (c) Dependence of the Faraday rotation angle on the relative frequency ω/ω_0 at $\alpha = 0.2$. (d) Dependence of the Faraday rotation ellipticity on the relative frequency ω/ω_0 at $\alpha = 0.2$.

see that both the Faraday rotation angles and ellipticity are shown to change abruptly at some frequency region. We find that the frequency region with the sudden change of θ_f and η_f is consistent with the frequency region where the system shows the left-handed property. When $\alpha > \alpha_c$, the drastic changes of θ_f and η_f disappear, where α_c is the critical parameter that determines the material's transition from left-handed to right-handed properties at a given filling factor. This character is expected to be a technical method to identify the left-handed properties of magnetic material. We also discuss the influence of the thickness of the film on the Faraday rotation angle. In usual thin magnetic garnet materials, the Faraday rotation angle is quite small, thus, a very large thickness is needed for the application of magneto-optical devices [7, 24]. However, in our model, we find that the increase of thickness of the film causes the decrease of θ_f . The result, in Figure 5a, shows the the Faraday rotation angles versus the the relative frequency ω/ω_0 under the different thicknesses of the film with $d = 0.1, 0.2, 0.3 \mu\text{m}$. We can see the Faraday rotation angles are on the decrease when the thickness of the film increases. The thinner the film is, the larger θ_f is obtained. So if we want to get the large Faraday rotation angle, it is disadvantage to use thick ferromagnetic film from our calculation. For comparison with the pure ferromagnetic film, we plot the Faraday rotation angle versus the relative frequency ω/ω_0 for our composite and the pure ferromagnetic film in Figure 5b. The solid line and

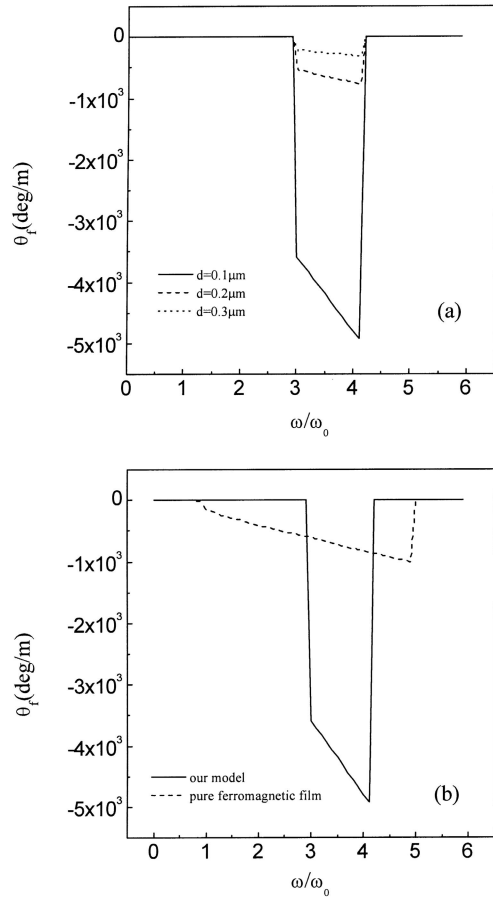


Fig. 5. (a) The Faraday rotation angles versus the relative frequency ω/ω_0 at the different thickness of the composite film $d = 0.1, 0.2, 0.3 \mu\text{m}$. (b) The Faraday rotation angles versus the relative frequency ω/ω_0 for our composite and a pure ferromagnetic film. The solid line represents the values of ferromagnetic nanowires composite and the dash line represents the values of a pure ferromagnetic film.

the dash line stand for our model with randomly arranged ferromagnetic nanowires in a nonmagnetic host and the pure ferromagnetic film, respectively. From Figure 5b, we can see that our model has much larger θ_f than that of the pure ferromagnetic film at a certain frequency region. To obtain large Faraday rotation angle, therefore, the fabrication of thin ferromagnetic nanowires composite is superior to the pure ferromagnetic thin film.

4 Conclusions and discussions

In this paper, we suggest an alternate ferromagnetic nanowires composite which can realize left-handed property at proper frequency range and provide a description of magneto-optical properties in such a composite. Here we would like to mention that the ferromagnetic nanowires in our model may be metallic magnetic materials, whose dielectric permittivity and magnetic permeability usually possess the forms of equation (9). The ferromagnetic reso-

nance frequency of such metallic magnetic materials usually lies in the microwave frequency region. Our results demonstrate that the composite may be left-handed when the damping factor satisfies a certain condition and this condition is affected by the filling factor of ferromagnetic nanowires. Based on the 4×4 transfer matrix method, the magneto-optical properties of left-handed material are calculated. According to our results, we find that there exist Faraday rotation angle and Faraday rotation ellipticity in such left-handed material and they exhibit anomalous behaviors near the ferromagnetic resonance frequency. At the frequency region where the composite exhibits left-handed property near the ferromagnetic resonance frequency both the Faraday rotation angle and ellipticity of the film show obvious change. This character is expected to be a technical method to identify the left-handed properties of magnetic material. The influence of the thickness of the film on the Faraday rotation angles is also investigated at the frequency region where the magnetic film is left-handed. With the increase of the thickness of the film, the Faraday rotation angle decreases. The thinner the film is, the larger θ_f is obtained. Our result shows that a larger Faraday rotation angle can be obtained by our model in comparison with a pure ferromagnetic film. We expect our composite may be advantage for technique application with its characteristic of low energy losses and large Faraday rotation angle.

This project was supported by the National Natural Science Foundation of China under Grant No. 10304013 and Jiangsu provincial Education Foundation under Grant No. 03KJB140119. We would like to thank Dr. Galina Kraftmakher for useful discussions.

References

1. B. Koopmans, M. van Kampen, J.T. Kohlhepp, W.J.M. de Jonge, *Phys. Rev. Lett.* **85**, 844 (2000)
2. V.V. Pavlov, R.V. Pisarev, A. Kirilyuk, Th. Rasing, *Phys. Rev. Lett.* **78**, 2004 (1997)
3. F.A. Pinheiro1, A.S. Martinez, L.C. Sampaio1, *Phys. Rev. Lett.* **84**, 1435 (2000)
4. M. Abe, T. Suwa, *Phys. Rev. B* **70**, 235103 (2004)
5. N.A. Yusuf, J. Shobaki, H. Abu-Safia, I. Abu-Aljarayesh, *J. Magn. Magn. Mater.* **149**, 0373 (1995)
6. M. Rasa, A.P. Philipse, D. Jamon, *Phys. Rev. E* **68**, 031402 (2003)
7. H. Kato, T. Matsushita, A. Takayama, M. Egawa, K. Nishimura, M. Inoue, *J. Appl. Phys.* **93**, 3906 (2003)
8. M. Inoue, K. Arai, T. Fujii, M. Abe, *J. Magn. Soc. Jpn* **23**, 1861 (1999)
9. S. Sakaguchi, N. Sugimoto, *Opt. Commun.* **162**, 64 (1999)
10. D.R. Smith, Willie J. Padilla, D.C. Vier, S.C. Nemat-Nasser, S. Schultz *Phys. Rev. Lett.* **84**, 4181 (2002)
11. R.A. Shelby, D.R. Smith, S. Schultz, *Science* **292**, 77 (2002)

12. V.G. Veselago, *Sov. Phys. USPEKHI* **10**, 509 (1968)
13. S.T. Chui, Liangbin Hu, *Phys. Rev. B* **21**, 2248 (1980)
14. S.T. Chui, Z.F. Lin, L.B. Hu, *Phys. Lett. A* **319**, 85 (2003)
15. R.X. Wu, Xiaokai Zhang, Z.F. Lin, S.T. Chui, John Q. Xiao, *J. Magn. Magn. Mater.* **271**, 180 (2004)
16. A. Figotin, I. Vitebskiy, *Phys. Rev. B* **67**, 165210 (2003)
17. A. Figotin, I. Vitebskiy, *Phys. Rev. E* **63**, 066609 (2001)
18. G. Goglio, S. Pignard, A. Radulescu, L. Piraux, I. Huynen, D. Vanhoenacker, A. Vander Vorst, *Appl. Phys. Lett.* **75**, 1769 (1999)
19. L. Piraux, J.M. George, J.F. Despres, C. Leroy, E. Ferain, R. Legras, K. Ounadjela, A. Fert, *Appl. Phys. Lett.* **65**, 2484 (1994)
20. W. Wernsdorfer, B. Doudin, D. Maily, K. Hasselbach, A. Benoit, J. Meier, J.P. Ansermet, B. Barbara, *Phys. Rev. Lett.* **77**, 1873 (1996)
21. A. Saib, D. Vanhoenacker-Janvier, I. Huynen, A. Encinas, L. Piraux, E. Ferain, R. Legras, *Appl. Phys. Lett.* **83**, 1769 (1999)
22. P.M. Hui, D. Stroud, *Appl. Phys. Lett.* **50**, 950 (1987)
23. Ping Xu, Tian-Yi Cai, Zhen-Ya Li, *Solid State Commun.* **130**, 451 (2004)
24. M. Inoue, K. Arai, T. Fujii, M. Abe, *J. Appl. Phys.* **83**, 6768 (1998)